Leakage properties of photonic crystal fibers

D. Ferrarini, L. Vincetti, M. Zoboli

Universty of Modena and Reggio Emilia, Dipartimento di Ingegneria dell'Informazione, Via Vignolese 905, I-41100 Modena, Italy

zoboli.maurizio@unimore.it; vincetti.luca@unimore.it
http://www.dii.unimo.it

A. Cucinotta, S. Selleri

University of Parma, Dipartimento di Ingegneria dell'Informazione, Parco Area delle Scienze 181/A, I-43100 Parma, Italy

annamaria.cucinotta@unipr.it; stefano.selleri@unipr.it
http://www.dii.unipr.it

Abstract: An analysis of the confinement losses in photonic crystal fibers due to the finite numbers of air holes is performed by means of the finite element method. The high flexibility of the numerical method allows to consider fibers with regular lattices, like the triangular and the honeycomb ones, and circular holes, but also fibers with more complicated cross sections like the cobweb fiber. Numerical results show that by increasing the number of air hole rings the attenuation constant decreases. This dependence is very strong for triangular and cobweb fibers, whereas it is very weak for the honeycomb one.

© 2002 Optical Society of America

OCIS codes: (060.2400) Fiber properties; (060.2280) Fiber design and fabbrication

References and links

1. T. P. White, R. C. McPhedram, C. M. de Sterke, L. C. Botten, and M. J. Steel, "Confinement losses in microstructured optical fibers," Opt. Lett. **26**, 1660-1662 (2001).
2. V. Finazzi, T. M. Monro, and D. J. Richardson, "Confinement losses in highly nonlinear holey optical fibers," in Optical Fiber Communication 2002, vol. 70 of OSA Trends in Optics and Photonics Series (Optical Society of America, Washington, D.C. 2002), paper ThS4.
3. K. Saitoh, and M. Koshiba, "Full-vectorial imaginary-distance beam propagation method based on a finite element scheme: application to photonic crystal fibers," IEEE J. Quantum Electron. **38**, 927-933 (2002).
4. A. Cucinotta, S. Selleri, L. Vincetti, and M. Zoboli, "Perturbation analysis of dispersion properties in photonic crystal fibers through the finite element method," J. Lightwave Technol. **20**,(2002).
5. A. Cucinotta, S. Selleri, L. Vincetti, and M. Zoboli, "Holey fiber analysis through the finite element method," IEEE Photon. Technol. Lett. **14**, 1530-1532 2002.
6. S. Selleri, L. Vincetti, A. Cucinotta, and M. Zoboli, "Complex FEM modal solver of optical waveguides with PML boundary conditions," Opt. Quantum Electron. **33**, 359-371 (2001).
7. J.C. Knight, J. Arriaga, T.A. Birks, A. Ortigosa-Blanch, W.J. Wadsworth and P. St. Russell, "Anomalous dispersion in photonic crystal fiber," IEEE Photon. Technol. Lett., **12**, 807-809 (2000).
8. S. E. Barkou, J. Broeng, and A. Bjarklev, "Dispersion properties of photonic bandgap guiding fibers," in Optical Fiber Communication Conference , OSA Technical Digest (Optical Society of America, Washington DC, 1998), FG5.
9. A. Ferrando, E. Silvestre, P.Andrés, J. J. Miret, and M. V. Andrés, "Designing the properties of dispersion-flattend photonic crystal fibers," Opt. Express **9**, 687-697 (2001). http://www.opticsexpress.org/abstract.cfm?URI=OPEX-9-13-687

1   Introduction

Photonic crystal fibers (PCFs) guide the electromagnetic field by means of an arrangement of air holes that run down the entire fiber length. In the holey fibers the air holes reduce the average index around the solid core and the guidance can be ascribed to the total internal reflection. Conversely in the photonic band gap fibers the average core index could be lower than the average cladding index and the guidance is due to the photonic band gap in the transverse direction. In both cases a lossless propagation is possible only if the air hole arrangement is of infinite extent and, of course, if a lossless material is used. In practice, a finite numbers of holes can be made and so the modes of such fibers are leaky. Furthermore the material introduces losses due to absorption and to Rayleigh scattering. If the latter cannot be eliminated, the former can be reduced by means of a proper design. Thus a fiber can be seen as confinement lossless if the field leakage is negligible with respect to the material losses. To investigate leaky modes properties, in order to find guidelines for the design of lossless fibers, numerical models with proper boundary conditions must be adopted. In fact, periodic boundary conditions or perfect electric or magnetic conductor boundary conditions which usually are employed in the numerical models affect the transverse Poynting vector flow of the numerical solutions. Recently the multipole method has been proposed to investigate losses in microstructured fibers [1]. This method, based on cylindrical function expansion, is useful when the holes are circular and it has been successfully applied to investigate confinement losses in fibers with a triangular lattice [1], [2]. The same kind of fiber has been also investigated through the finite element method (FEM) based on the imaginary distance technique and using perfectly matched layers (PML) as boundary conditions [3]. The finite element method is a useful tool to analyze PCFs. It has been already successfully applied to investigate dispersion properties of triangular and cobweb PCFs [4], [5]. The fiber cross section representation is very accurate as the domain is divided into sub-domains with triangular or quadrilateral shape where any refractive index profiles can be properly represented. Unfortunately, the imaginary distance approach is time-consuming as it calculates just one mode for each run through a iterative procedure [3]. A FEM formulation for modal analysis based on anisotropic perfectly matched layers able to calculate as many modes as desired in a single run without setting any iterative procedure has been recently presented and applied to the analysis of leaky modes in antiresonant reflecting optical waveguides [6]. In this work this formulation is applied to the analysis of the leakage properties of holey fibers with both circular and non-circular holes as well as photonic band gap fibers. Triangular, honeycomb and cobweb PCFs have been analyzed by changing number, size, and pitch of holes as well as the wavelength. Despite their interesting applications, to authors' knowledge, data about losses in photonic band gap fibers as well as cobweb fibers has been not published yet. The results show that with a proper design, fibers with confinement losses negligible with respect to those due to the medium can be obtained for both triangular and cobweb fibers. On the contrary it has been observed that honeycomb fiber exhibits high loss also with cross section having many air holes.

2   The Finite Element Method Formulation

Both electric field and magnetic field based formulations can be developed. Here for the sake of simplicity a magnetic field formulation is presented. The reader can find more details in [6]. The formulation starts from the curl-curl equation obtained decoupling the Maxwell equations:

$$\overline{\nabla} \times (\overline{\overline{\varepsilon}}_r^{-1} \overline{\nabla} \times \overline{h}) - k_0^2 \overline{\overline{\mu}}_r \overline{h} = 0 \tag{1}$$

where $\overline{h}$ is the magnetic field, $\overline{\overline{\varepsilon}}_r$ and $\overline{\overline{\mu}}_r$ are the relative dielectric permittivity and magnetic permeability complex tensors, respectively, and $k_0 = 2\pi/\lambda$ the wave number in the vacuum, λ being the wavelength. The magnetic field of the modal solution is expressed as $\overline{h} = \overline{H}e^{-\gamma z}$ where $\overline{H}$ is the field distribution on the transverse plane and $\gamma = \alpha + j\beta$ is the complex propagation constant with α the attenuation constant and β the phase constant. By applying the variational finite element procedure, the full vector equations (1) yields the algebraic problem [6]:

$$([A] - (\frac{\gamma}{k_0})^2[B])\{H\} = 0$$

where the eigenvector $\{H\}$ and the eigenvalue $(\frac{\gamma}{k_0})^2$ provide, respectively, the full vectorial magnetic field distribution and the effective index of the mode. In the present formulation triangular high order edge elements have been used. In order to enclose the computational domain without affecting the numerical solution, anisotropic perfectly matched layers are placed before the outer boundary. This formulation is able to deal with anisotropic material both in terms of dielectric permittivity and magnetic permeability allowing anisotropic PMLs to be directly implemented. Furthermore fiber symmetry can be used to reduce the computational domain and consequently both time and memory required.

3 Results

3.1 *Triangular fiber*

The PCF first considered in the analysis consists of a triangular lattice of air holes. An example of its cross section is reported in figure 1(a) in the case of four rings. The different colors show different rings. Figure 1(b) shows the magnetic field main component of one of the two polarizations of the fundamental mode. The fiber considered consists of two rings of holes having diameter $d = 0.69\mu m$ and pitch $\Lambda = 2.3\mu m$. Notice that due to fiber symmetry just a quarter of the cross section can be considered for the analysis. The hexagonal symmetry as well as the leakage due to the interruption of the lattice are evident. The field confinement and its decay rate play a fundamental role in
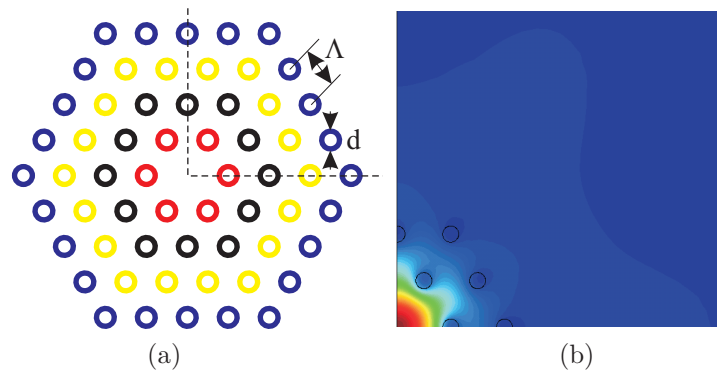

(a)   (b)

Fig. 1. (a): triangular fiber with four hole rings. The lines with different colors show different rings: black first ring, red second one, yellow third one, and blue fourth one. The dashed lines shows the quarter of the structure considered in the analysis. (b): main component of the magnetic field for a fiber having two rings, $d/\Lambda = 0.3$ and $\Lambda = 2.3\mu m$.

the leakage properties. They depend on the hole diameter, on their pitch and on the number of rings. Figure 2 shows the losses versus the diameter d normalized to the pitch

value $\Lambda = 2.3\mu m$. As expected, the losses quickly decrease by increasing the numbers of rings and the hole diameter. Also the slope increases with these parameters. In fact, with $d = 0.69\mu m$, that is $d/\Lambda = 0.3$, going from a ring to eight rings losses decrease from $10^5 dB/m$ to a value a little lower than $10 dB/m$. Notice that this corresponds to pass from six to two hundred and sixteen holes. By increasing the hole diameter to $d = 0.92\mu m = 0.4\Lambda$, the upper value of the range goes to $0.5 \times 10^5 dB/m$, whereas the lower value goes to 10^{-5} which is negligible with respect to all the other causes of losses, like to absorption and the Rayleigh scattering. Figure 2(b) shows that a loss reduction is also obtained by fixing the ratio d/Λ and by increasing the pitch Λ. The pitch and the hole diameter are changed of the same scale factor, consequently greater pitches correspond to greater core size and thus more confined fields. Specific dispersion profile can be obtained playing on ratio d/Λ and on the scale factor [9]. Thus, the dependence on these parameters is very important to design fibers with a good trade-off between the dispersion and loss properties. In this frame, another important aspect to investigate
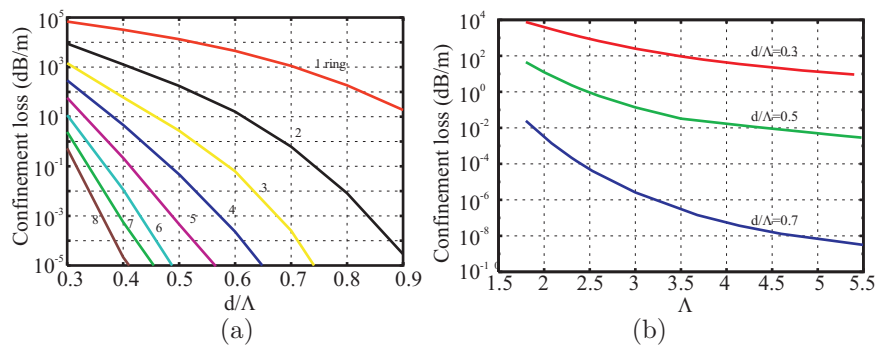

Fig. 2. (a): confinement loss as a function of hole diameter d normalized to pitch $\Lambda = 2.3\mu m$ for different numbers of rings. (b): confinement loss as a function of pitch Λ for different ratios d/Λ. In both cases a wavelength $\lambda = 1.55\mu m$ is assumed

is the wavelength dependence. Figure 3 shows the results of this analysis. As expected, the losses increase with the wavelength because the field confinement decreases. The numbers of rings still affects this dependence. For few rings the dependence is weak, whereas for many rings it becomes stronger. Passing from $1300 nm$ to $1700 nm$ with one ring, the losses are almost wavelength-independent, conversely, with five rings, the losses increase of about two orders of magnitude. This variation decreases of one order going from a pitch $\Lambda = 2.3\mu m$ to a pitch $\Lambda = 4.6\mu m$. In fact greater pitches correspond to larger cores and thus more confined fields. As a consequence, a wavelength increment corresponds to a little increment of the confinement with a little reduction of the losses.

3.2 *Honeycomb fiber*

It is very interesting also to investigate the loss phenomena in fibers where guiding can be ascribed to photonic band gap as, for example, the honeycomb fibers. The cross section of the honeycomb fiber considered in the analysis is reported in figure 4(a). The defect consists on a extra hole with the same diameter as that of the lattice holes. The holes belonging to different rings are highlighted with different colors. Notice that in this kind of fiber the number of holes increases with the number of rings more quickly than in the triangular one. Passing from two to three rings in a triangular fiber the numbers of holes pass from eighteen to thirty-six while in a honeycomb they pass from fifty-four to ninety-six. However, due to the lower air filling factor, that is the ratio
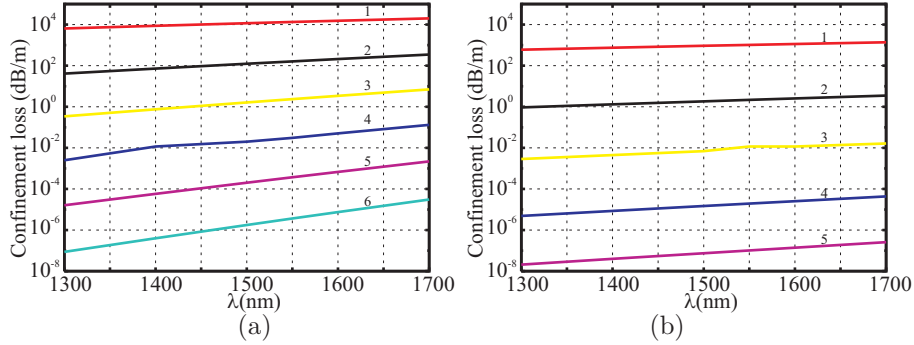
Fig. 3. Confinement loss as a function of the wavelength λ for different numbers of rings and $d/\Lambda = 0.5$. (a) $\Lambda = 2.3\mu m$; (b) $\Lambda = 4.6\mu m$
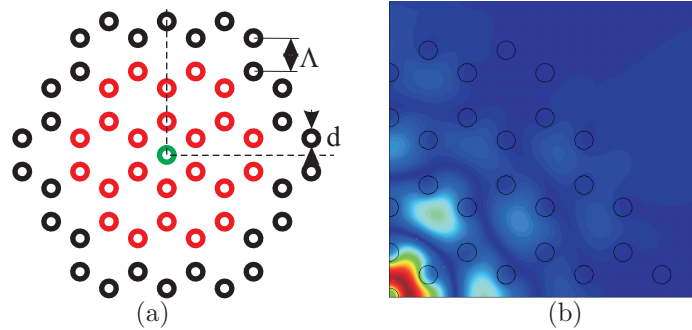

Fig. 4. (a): honeycomb fiber with three hole rings. The circles with different colors show different rings: red first ring and black second one. The dashed lines shows the quarter of the structure considered in the analysis. (b): fundamental mode profile of a honeycomb fiber having three rings and $d/\Lambda = 0.41$ at the wavelength $\lambda = 1.55\mu m$.

between the areas of the air holes and the unitary cell, the mode is less confined as shown in figure 4(b). This causes higher losses and above all a weaker dependence on the number of rings. Figure 5(a) shows this aspect. Comparing the results of figure 5 and 2, for few rings, the losses are a little bit higher than those of the triangular fiber, but by increasing the rings the difference grows reaching six orders of magnitude for eight rings. As a consequence in the considered fibers, the losses are always higher than $10dB/m$. The figure also shows another important difference with respect to the triangular fiber. Higher ratios d/Λ exhibit lower losses only up to six rings, after that the losses slightly increase. This can be ascribed to the fiber guidance mechanism. In fact the lattice of the fiber determines a truly photonic band gap only if the number of rings is very high. Also the wavelength dependence, shown in figure 5(b), is weaker than in the triangular one. It slightly increases with ring numbers and it reaches a order of magnitude with nine rings, over the wavelength range here considered.

3.3   *Cobweb fiber*

Finally the cobweb fiber is considered. This fiber is very interesting for its small effective area [7] and very high negative dispersion [5]. It consists of a aperiodic arrangement of non-circular air holes. Figure 6(a) shows the cross section of two cobweb fibers having one and three rings, respectively at the top and at the bottom. The thickness of the silica bridges which separate the holes is about $120nm$. This low value combined with very large holes assures very low losses as showed in figure 6(b). The wavelength dependence is stronger than in the previous fibers and it increases by increasing the number of rings.
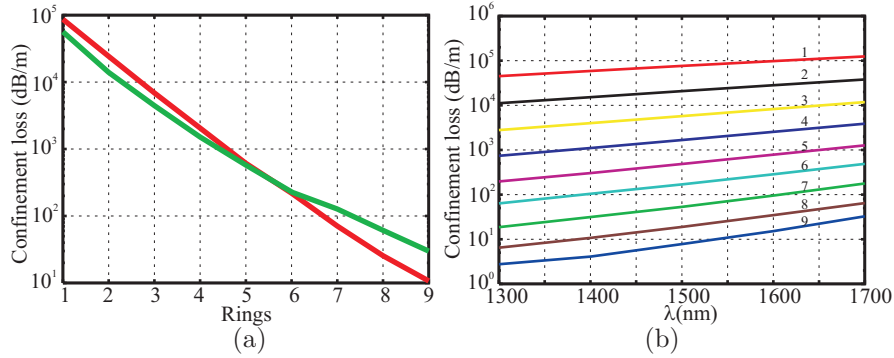
Fig. 5. (a): confinement loss as a function of numbers of rings at the wavelength $\lambda = 1.55\mu m$ and for $d/\Lambda = 0.41$ red line and for $d/\Lambda = 0.55$ green line. (b): confinement loss as a function of the wavelength λ for different numbers of rings and $d/\Lambda = 0.41$. In both cases $\Lambda = 1.62\mu m$ is assumed.
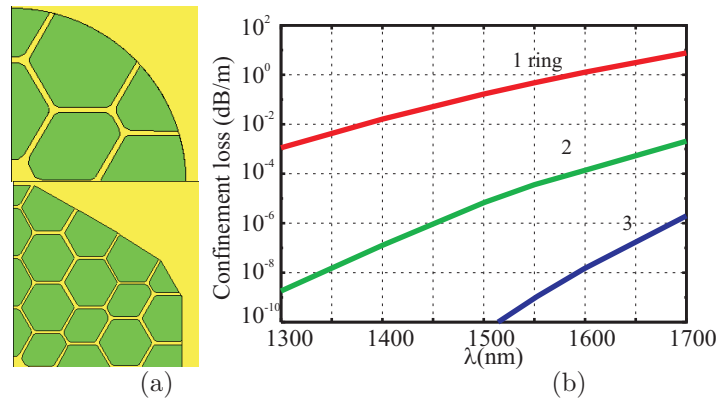

Fig. 6. (a): cross sections of the cobweb fiber with one (top) and three (bottom) rings. (b): confinement loss as a function of the wavelength for different ring numbers.

For two rings, passing from $1300nm$ to $1700nm$ of wavelength, the losses change of six orders of magnitude. However, for all wavelengths here considered, with just three rings the losses are lower than $10^{-5}dB/m$. The losses are due mainly to the field which passes through the silica bridges.

4   Conclusion

In this work confinement losses in PCFs have been analyzed through a modal solver based on the finite element method. Three kinds of PCFs have been considered. PCFs with triangular lattice and the cobweb fiber show a strong dependence of the confinement losses on the number of rings, especially for high air filling factor. This allows to obtain fibers with confinement losses negligible with respect to those given by the medium. Also, by increasing the pitch the losses decrease. Conversely confinement losses in honeycomb fibers exhibit a weaker dependence on the number of rings and the air filling factor. However for this fiber and for the considered number of rings, the losses are always higher than $10dB/m$, values which could affect their applications. Several aspects, like the role of the bridge thickness in the cobweb fibers, the dimension of the central defect in honeycomb fibers or the influence of the confinement losses on dispersion parameters, must be still investigated and will be the object of future works.